

# X-ray excited luminescence of SrAl<sub>2</sub>O<sub>4</sub>:Eu,Dy at low temperatures

V. Liepina, D. Millers<sup>\*</sup>, K. Smits, A. Zolotarjovs, I. Bite

*Institute of Solid State Physics, University of Latvia, Latvia*

## 1. Introduction

SrAl<sub>2</sub>O<sub>4</sub>:Eu,Dy is a very efficient green-emitting phosphor, its long-lasting afterglow can be observed up to 30 h after the termination of excitation [1]. Therefore, SrAl<sub>2</sub>O<sub>4</sub>:Eu,Dy is promising for a wide range of applications – emergency signage, watch dials, luminous paints, in vivo imaging [2–4]. There are a lot of studies already completed on this material - the intense research is focused on clearing up the ambiguities of long-lasting afterglow mechanism and identifying the charge carrier traps. There is strong evidence confirming the fact that Eu<sup>2+</sup> is the luminescence center responsible for the blue/green emission [5–9]. The Eu<sup>2+</sup> changes its charge state during excitation, the electron from Eu<sup>2+</sup> is transferred to some unidentified trap [10–12] and a number of traps are filled. The gradual thermally stimulated release of electrons from traps takes place at room temperature (RT). The released electrons recombine with Eu<sup>3+</sup> ion, thus resulting in excited Eu<sup>2+</sup> creation. The following radiative transition to the Eu<sup>2+</sup> ground state is the origin of the green luminescence observed [8,12,13]. However, in addition to thermally stimulated process, the creation of excited Eu<sup>2+</sup> luminescence center via electron tunneling was observed recently as well [14]. Thus, both processes can contribute in creation of an excited Eu<sup>2+</sup> luminescence center. The role of co-dopant Dy<sup>3+</sup> is disputable up to now and surprising is that we find only two studies of only Dy<sup>3+</sup> doped aluminates luminescence [15,16].

Most of the studies of long-lasting afterglow have been carried out for temperature range around RT [6] and above due to the possible applications of material. The studies of luminescence processes in SrAl<sub>2</sub>O<sub>4</sub>:Eu, Dy at low temperatures were not very frequent since the afterglow is very weak or not observed below 240 K after photoexcitation [6], and mainly photoluminescence is investigated, turning less attention to X-ray excited afterglow.

The low temperature studies, however, do reveal some interesting information – not one, but two luminescence bands peaking at 450 nm and 520 nm have been observed in luminescence spectrum of SrAl<sub>2</sub>O<sub>4</sub>:Eu,Dy at low temperatures; the 450 nm band undergoes thermal quenching in temperatures above 150 K. It should be noted the luminescence band close to 450 nm at RT was observed also in undoped SrAl<sub>2</sub>O<sub>4</sub> [17]. Various ideas concerning the origin of the 450 nm

luminescence band have been expressed [6,7,18,19]. The role of Eu<sup>2+</sup> ions was discussed within these ideas. The possible contribution of SrAl<sub>2</sub>O<sub>4</sub> intrinsic defects luminescence was not studied up to now. It is surprising that the afterglow of 450 nm luminescence is recorded only in microsecond range at low temperatures [7,10]. As the electron tunneling process is not temperature dependent, it would be expected that the afterglow at low temperatures could be observed for at least several seconds.

The luminescence spectra of X-ray excited SrAl<sub>2</sub>O<sub>4</sub>:Eu,Dy reveals additional luminescence peaks overlapping with Eu<sup>2+</sup> band [11,20,21] and these additional bands are attributed to Dy<sup>3+</sup> luminescence. The three Dy<sup>3+</sup> luminescence bands are mentioned in Ref. [11], whereas one Dy<sup>3+</sup> band is mentioned in Refs. [20,21]. Dy<sup>3+</sup> and Eu<sup>3+</sup> ions have emission peaks in relatively close positions, in luminescence spectrum of SrAl<sub>2</sub>O<sub>4</sub>:Eu,Dy the peaks of Eu<sup>3+</sup> are close to those of Dy<sup>3+</sup>.

We carried out the study of X-ray excited luminescence of SrAl<sub>2</sub>O<sub>4</sub>:Dy and SrAl<sub>2</sub>O<sub>4</sub>:Eu,Dy including the measurements of afterglow at low temperatures within extended time scale, as the results could elucidate details of luminescence process in this material. The luminescence of SrAl<sub>2</sub>O<sub>4</sub>:Eu,Dy under X-ray excitation reveals bands that could be Dy<sup>3+</sup> luminescence, accordingly the study of SrAl<sub>2</sub>O<sub>4</sub>:Dy was carried out to convincingly confirm the Dy<sup>3+</sup> contribution in SrAl<sub>2</sub>O<sub>4</sub>:Eu,Dy luminescence.

## 2. Experimental

The Sr<sub>0.97</sub>Al<sub>2</sub>O<sub>4</sub>:Eu<sub>0.01</sub>,Dy<sub>0.02</sub> powder and of Sr<sub>0.98</sub>Al<sub>2</sub>O<sub>4</sub>:Dy<sub>0.02</sub> powder were prepared by solid state reaction with stoichiometric amounts of Al(NO<sub>3</sub>)<sub>3</sub>, Sr(NO<sub>3</sub>)<sub>2</sub>, Eu(NO<sub>3</sub>)<sub>3</sub>, Dy(NO<sub>3</sub>)<sub>3</sub>. The mixture of components, including a minor addition of boric acid was heated at 1300 °C under a weak reductive carbon atmosphere. The structure of obtained powder was determined from XRD data using Bruker AXS GmbH DS Advance diffractometer. The estimated grain size from the XRD data was 55 μm. Energy dispersive X-ray spectroscopy (EDX) method was applied to determine the relative amounts of elements in the material. A YAG:Nd laser LCS-DTL-382QT (266 nm, 8 ns) was used for photoluminescence excitation. The samples were cooled down using Janis closed cycle refrigerator CCS-100 operating within temperature range ~9–325 K. The

<sup>\*</sup> Corresponding author.

E-mail address: [dmillers@latnet.lv](mailto:dmillers@latnet.lv) (D. Millers).

Lake Shore 331 Temperature controller was used for temperature control as well as for sample heating (6 deg/min) during thermally stimulated luminescence (TSL) measurements up to 320 K. A self-made heating equipment was used for TSL measurements within 295–650 K. Luminescence spectra were recorded using Andor Shamrock B303-I spectrometer. The integration time was set 1 m s for each spectrum recording. It is known that the filling of traps under UV excitation depends on both, the wavelength and temperature [6], indicating the energy necessary for the migration of charge carriers. Therefore, for successful trap filling at low temperature, the samples were irradiated by X-rays. The excitation source was X-ray tube with W target. The voltage of tube can be varied within 14kV-35kV and the current within 1–15 mA range, thus providing variable X-ray energy and intensity.

### 3. Results and discussion

#### 3.1. Sample characteristics

The EDX measurements for sample  $\text{Sr}_{(1-x-y)}\text{Al}_2\text{O}_4:\text{Eu}_x,\text{Dy}_y$  shows that the relative amounts of cations are: 0,927 Sr, 0,014 Eu and 0,036 Dy, and in sample  $\text{Sr}_{(1-y)}\text{Al}_2\text{O}_4:\text{Dy}_y$  - 0,95 Sr, and 0,049 Dy. Besides these dopants, a trace amount of Zr seems to be present in the material, possibly it appears because transient metals are usual impurities of  $\text{AlO}_3$ .

The XRD patterns of  $\text{SrAl}_2\text{O}_4:\text{Eu},\text{Dy}$  and  $\text{SrAl}_2\text{O}_4:\text{Dy}$  powders are shown in Fig. 1. Comparison of these XRD patterns with data from International Center for Diffraction Data (ICDD) Inorganic Crystal Structure Database [00-034-0379] confirms the dominant phase of both samples is monoclinic  $\text{SrAl}_2\text{O}_4$ , however a minor admixture of  $\text{Sr}_3\text{Al}_2\text{O}_6$  phase is detected. The estimated contribution of  $\text{Sr}_3\text{Al}_2\text{O}_6$  phase is close to 10% for sample  $\text{SrAl}_2\text{O}_4:\text{Eu},\text{Dy}$  and less than 5% for sample  $\text{SrAl}_2\text{O}_4:\text{Dy}$ .

We measured the photoluminescence spectrum of the  $\text{SrAl}_2\text{O}_4:\text{Eu},\text{Dy}$  and the position of  $\text{Eu}^{2+}$  luminescence band at room temperature (RT) for our sample is 526 nm and it is in agreement with  $\text{SrAl}_2\text{O}_4:\text{Eu},\text{Dy}$  luminescence described in a number of papers, thus the dominant luminescent properties of these samples can be attributed to the dopants in  $\text{SrAl}_2\text{O}_4$  monoclinic phase.

#### 3.2. Luminescence of $\text{SrAl}_2\text{O}_4:\text{Dy}$ .

First, we carried out the study of the strontium aluminate doped only with Dy to confirm the origin of emission line groups in  $\text{SrAl}_2\text{O}_4:\text{Eu},\text{Dy}$ . The emission spectrum of  $\text{SrAl}_2\text{O}_4:\text{Dy}$  sample under X-ray excitation is in Fig. 2.

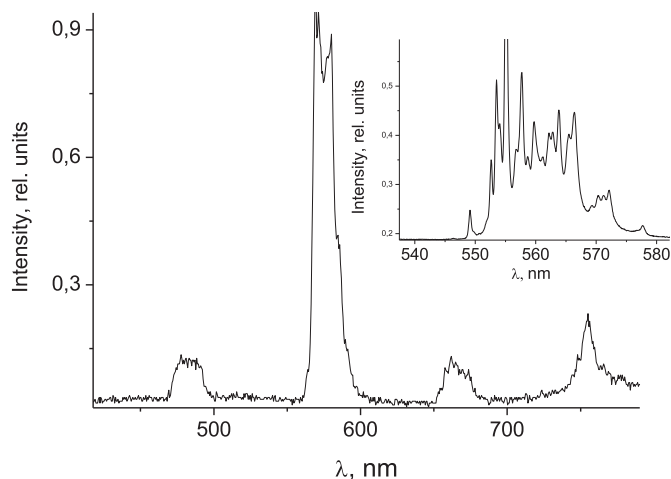


Fig. 2. Luminescence spectrum of  $\text{SrAl}_2\text{O}_4:\text{Dy}$  sample at 10 K.

There are four luminescence bands centered at  $\sim 483$  nm, 576 nm, 664 nm and 754 nm. The positions of these emission bands are close to those described in Refs. [16,20]. Nevertheless, the shapes of bands differ of those described in Ref. [16], where the luminescence bands are simple, but in our study the luminescence band shapes reveal a possible contribution from closely located and partially overlapping lines. These lines are barely resolved at RT, hence the spectrum was recorded at 10 K. The spectrum for more intense band at  $\sim 576$  nm in higher resolution is shown in inset in Fig. 2, and it reveals a group of emission lines. Since the interaction of  $\text{Dy}^{3+}$  with host matrix is weak [22] the luminescence spectra of  $\text{Dy}^{3+}$  ion should be similar in a number of materials and the spectrum can be compared with luminescence of  $\text{Dy}^{3+}$  in  $\text{YAG}:\text{Dy}$  [22] and  $\text{GdAlO}_3:\text{Dy}$  [23]. In these spectra, the sets of overlapping  $\text{Dy}^{3+}$  emission lines are in regions 460–500 nm, 550–610 nm and a low intensity band at 677 nm and this is very close to that observed in present study. Based on that, we conclude that the  $\text{SrAl}_2\text{O}_4:\text{Dy}$  under X-ray excitation exhibits only  $\text{Dy}^{3+}$  luminescence.

It is worth noting the intensity of  $\text{Dy}^{3+}$  luminescence at RT is more than twice of that at 10 K (Fig. 3), indicating that at 10 K only a fraction of X-ray generated electrons and holes undergoes recombination at  $\text{Dy}^{3+}$ . It can be assumed, that the other fraction of charge carriers are trapped at defects, for confirmation the measurements of TSL were conducted. The TSL glow curve of  $\text{SrAl}_2\text{O}_4:\text{Dy}$  is presented in Fig. 4 and three major glow peaks are observed at 110 K, 270 K and 532 K.

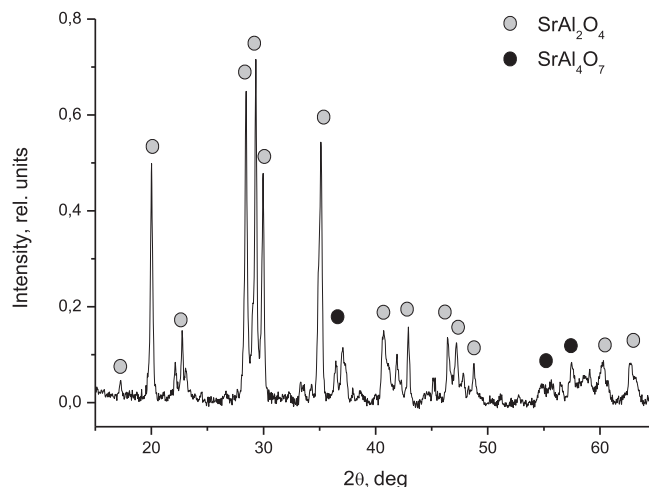
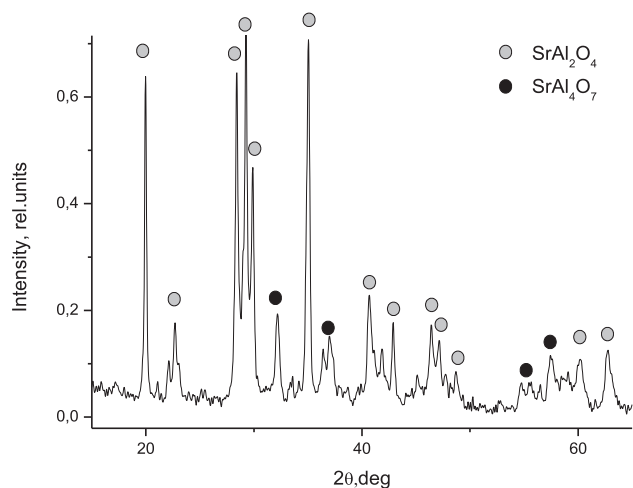


Fig. 1. XRD pattern of  $\text{SrAl}_2\text{O}_4:\text{Eu},\text{Dy}$  (a) and  $\text{SrAl}_2\text{O}_4:\text{Dy}$  (b) sample.

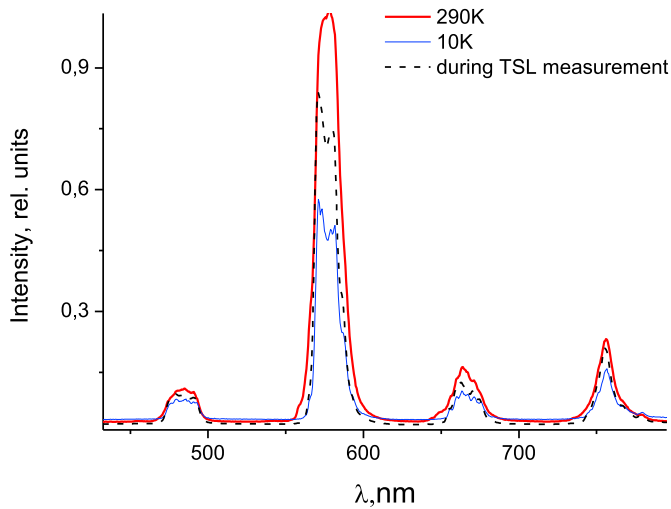


Fig. 3. Spectra of SrAl<sub>2</sub>O<sub>4</sub> under excitation at 10 K and room temperature and the spectrum during TSL measurement.

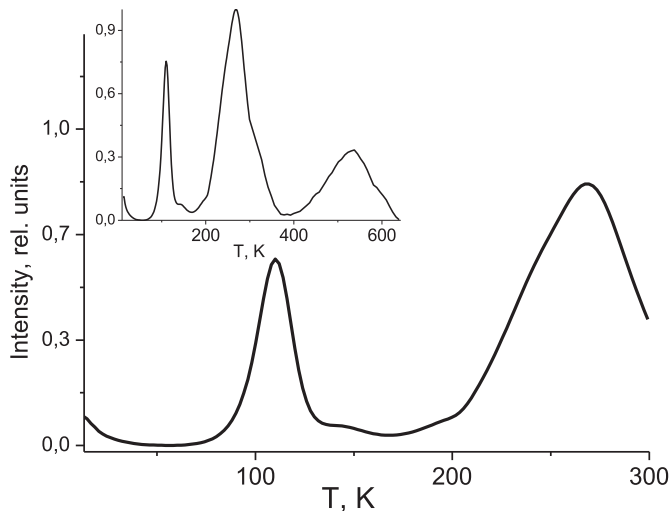


Fig. 4. X-ray induced TSL of SrAl<sub>2</sub>O<sub>4</sub>:Dy sample. Inset – larger scale.

The luminescence spectra in all the glow peaks coincide with the emission spectrum under X-ray excitation at 10 K (Fig. 3), meaning that only Dy<sup>3+</sup> luminescence bands were observed in TSL without the contribution from any other luminescence. There is one more thing in the TSL spectrum that requires clarification - the low temperature part of the measurement, where gradual decrease in the glow intensity is observed is not an additional TSL maximum in the low temperature range, but coincides well with the afterglow decay of glow intensity in time, that is discussed below. Therefore, we can assume there are no shallow traps, which release charges within the temperature range 10–60 K.

Another finding at 10 K temperature is the afterglow of this material at 576 nm (the more intense lines of Dy<sup>3+</sup> luminescence). The afterglow intensity as well as its decay kinetics are excitation duration time dependent, as it can be seen in Fig. 5. The afterglow decay kinetics are not simple exponential functions, as it is seen in the inset of Fig. 5.

The afterglow decay dependence on excitation time is additional evidence to the fact that during excitation accumulation of trapped charges takes place. The afterglow of several minutes at 10 K is not due to thermal release of charge carriers from traps, as discussed beforehand. Therefore, the origin of this afterglow is the excited Dy<sup>3+</sup> creation via electron tunneling. The TSL and afterglow are strong evidences that under X-ray irradiation the Dy<sup>3+</sup> ions undergo a charge state change. It

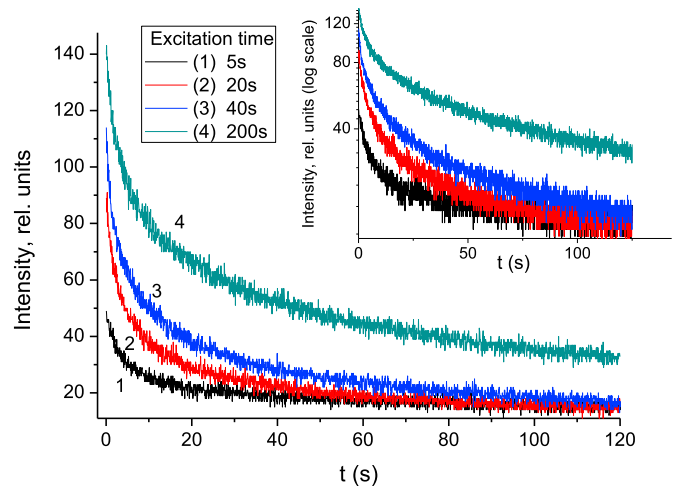


Fig. 5. The Dy<sup>3+</sup> afterglow decay for different excitation time intervals. Inset – afterglow decay in logarithmic scale.

should be pointed out that in the study of SrAl<sub>2</sub>O<sub>4</sub>:Eu,Dy under X-ray irradiation at 120 K the change of Eu<sup>2+</sup> charge was observed, not any change of Dy<sup>3+</sup> charge [11].

### 3.3. Luminescence of SrAl<sub>2</sub>O<sub>4</sub>:Eu,Dy

We recorded the luminescence spectra of SrAl<sub>2</sub>O<sub>4</sub>:Eu,Dy under excitation and during TSL measurement as well as the afterglow spectra. The luminescence spectra of sample SrAl<sub>2</sub>O<sub>4</sub>:Eu,Dy at RT after different excitation time are shown in Fig. 6. The spectra reveal the intense Eu<sup>2+</sup> luminescence band peaking at 526 nm, and three Dy<sup>3+</sup> luminescence bands peaking at 576 nm, 664 nm, 754 nm. The Dy lines are not visible in photoluminescence spectrum. The Dy<sup>3+</sup> band peaking at 483 nm is not resolved due to overlapping with intense wide Eu<sup>2+</sup> luminescence band. The shape of the spectrum changes during excitation and this could be due to gradual filling of traps by charge carriers. The luminescence intensity dependence on excitation time for several excitation intensities of X-Ray were recorded at RT and was observed that luminescence intensity saturation is delayed relative to the beginning of excitation (Fig. 7).

The similar luminescence intensity rise at RT was observed under UV excitation [6] as well as under X-ray excitation [11] and is explained as the thermally stimulated charge migration [6,11].

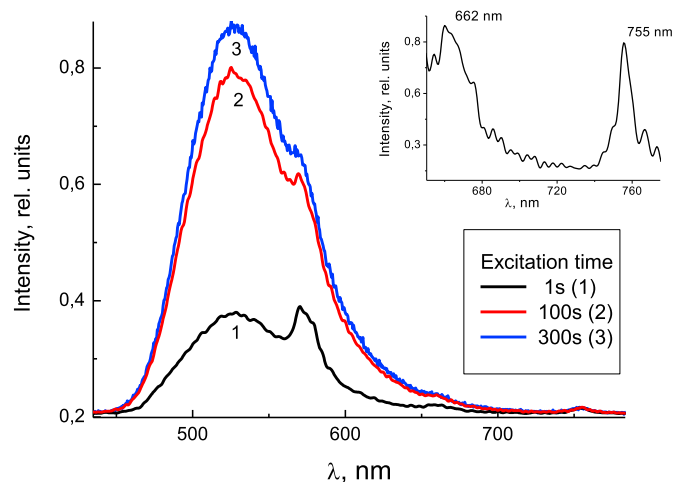


Fig. 6. Luminescence spectra of SrAl<sub>2</sub>O<sub>4</sub>:Eu,Dy for different excitation duration at RT Inset the 630–800 nm range in extended scale.

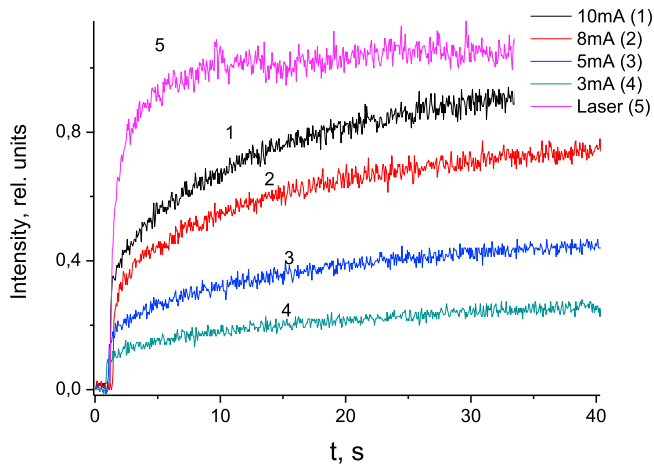


Fig. 7. The luminescence intensity at 526 nm dependence on excitation time at RT with different excitation energies with X-Ray and laser.

The analysis of luminescence spectra in Fig. 6 allowed to estimate that the changes of  $Dy^{3+}$  luminescence intensity during excitation are opposite to that observed for  $Eu^{2+}$  luminescence. The reason of this change yet unclear and additional investigation is necessary.

The spectra of X-ray and laser excited luminescence of  $SrAl_2O_4:Eu,Dy$  at low temperature are compared in Fig. 8. Under X-ray excitation both  $Dy^{3+}$  and  $Eu^{2+}$  luminescence is observed, whereas in photoluminescence spectrum only the well known  $Eu^{2+}$  broad band is visible – and it is the same as under X-ray excitation. The  $SrAl_2O_4:Eu,Dy$  was excited by X-ray for 10 min at 10 K and the afterglow spectra were recorded for different delay after X-ray termination (Fig. 9). These spectra reveals the same bands as spectrum under X-ray excitation. What is notable is that the afterglow of 455 nm blue band was observed in time range significantly exceeding microseconds in contrast to that observed in Refs. [7,8]. Also, the normalized afterglow spectra coincide well showing the decay rate of all luminescence bands was the same. There are two versions that could explain the same decay rate of all luminescence bands: (I) the luminescence decay is limited by the rate of thermally activated charge carrier release from some shallow traps; (II) the rare earth ions  $Eu^{2+}$  and  $Dy^{3+}$  luminescence in  $SrAl_2O_4$  is associated with similar defects which act as electron traps and excited  $Eu^{2+}$  and  $Dy^{3+}$  luminescence centers are created via electron tunneling. The verification of first version is simple:

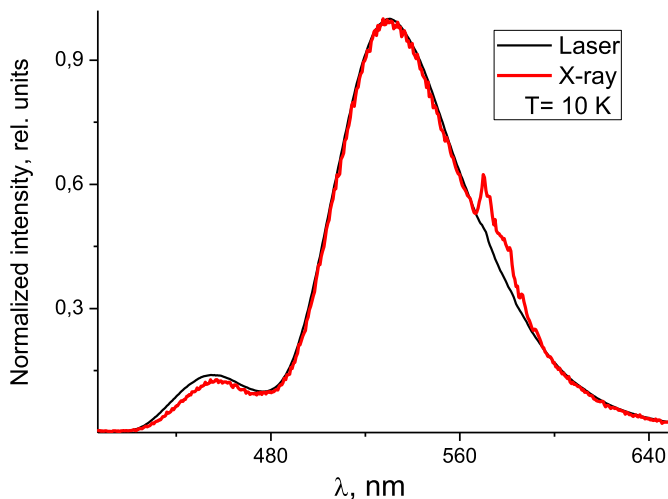


Fig. 8. Photoluminescence and X-ray excited  $SrAl_2O_4:Eu,Dy$  luminescence spectra.

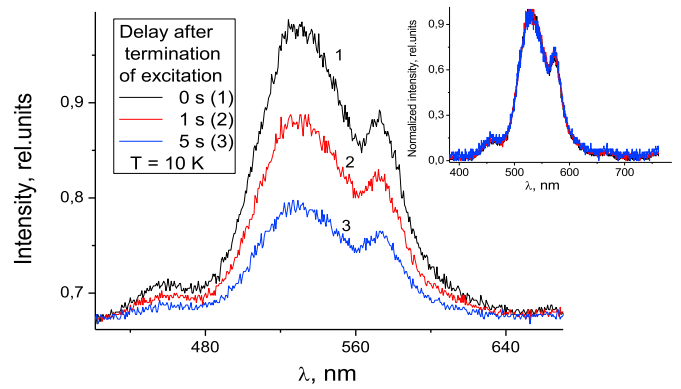


Fig. 9.  $SrAl_2O_4:Eu,Dy$  afterglow spectra at different time delay after X-ray Termination. Inset – normalized data.

the TSL of  $SrAl_2O_4:Eu,Dy$  sample irradiated by X-ray at 10 K can show if there is a glow peak close to 10 K. Therefore, the TSL curve and spectra in the glow peaks were recorded (Fig. 10).

The thermally stimulated glow curves, if we compare the  $SrAl_2O_4:Eu,Dy$  and  $SrAl_2O_4:Dy$  sample, differ considerably (see Figs. 4 and 10). The TSL peak at  $\sim 110$  K was observed in  $SrAl_2O_4:Dy$  as well as in undoped  $SrAl_2O_4$ , therefore it can be attributed to intrinsic defects. The  $Eu$  doping creates some other traps – the shallow one, responsible for TSL peak at 60 K and the traps responsible for TSL peak at  $\sim 140$  K and for peak slightly above room temperature. The latter overlaps with the peak in  $SrAl_2O_4:Dy$  slightly below room temperature. The glow curve in Fig. 10 shows low intensity peak between strong peaks at 60 K and 140 K, this peak position seems close to those observed at  $\sim 110$  K in undoped and only  $Dy$  doped  $SrAl_2O_4$ .

It is clear, that the trapping centers, created by rare earth doping - distorted tetrahedra of  $AlO_4$  - are similar, however not identical due to different  $Eu^{3+}$  and  $Dy^{4+}$  ion sizes and differently located energy levels of trapped electrons.

It is important to point out that there are no glow peaks within the temperature of 10–40 K – the weak tail of the first low temperature glow peak could be observed above 25 K. This suggests the origin of the afterglow recorded at 10 K can be due to the creation of excited  $Eu^{2+}$  and  $Dy^{3+}$  luminescence centers via electron tunneling. The TSL spectrum of  $SrAl_2O_4:Eu,Dy$  at 50 K is similar to that of afterglow at 10 K. It is generally accepted that during afterglow the excited  $Eu^{2+}$  center is created via  $Eu^{3+}$  recombination with electron [6,18]. Therefore, the glow peak at

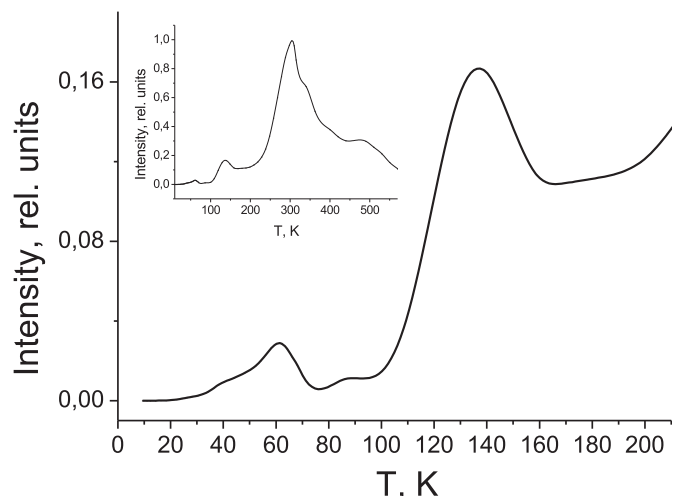


Fig. 10. T X-ray induced TSL of  $SrAl_2O_4:Eu,Dy$  sample. Inset – larger scale.

50 K corresponds to the thermal release of electrons from traps and the excited  $Dy^{3+}$  centers can appear due to  $Dy^{4+}$  recombination with electrons. The electrons were trapped at host defects; possibly at oxygen in distorted tetrahedra of  $AlO_4$  [24]. The important conditions for electron tunneling are: (I) the electron wave functions must overlap for electron initial and final state; (II) the energy of electron in initial and final state is equal. Experiments and corresponding calculations give confirmation that electron traps are located close to  $Eu^{3+}$  [6,13,14] and  $Dy^{4+}$  [24]. This suggests that wave function overlapping can take place and it is favorable for electron tunneling. The estimated energy levels for Eu and Dy ions in  $SrAl_2O_4$  differ [5,10,12], therefore one can suggest the depth of electron traps could differ also. On the other hand it seems that initially both Eu and Dy in  $SrAl_2O_4$  incorporate in charge states  $3+$  and the thermal treatment under reducing atmosphere leads to the formation of  $Eu^{2+}$ , but not the reduction of  $Dy^{3+}$ . The initial incorporation of  $Eu^{3+}$  and  $Dy^{3+}$  in  $SrAl_2O_4$  requires charge compensation by host defects and since the charge states of both dopants are the same, the same host defects can be created. The electron traps - distorted tetrahedra of  $AlO_4$  - are similar, however, not identical due to different  $Eu^{3+}$  and  $Dy^{4+}$  ion sizes and differently located energy levels of trapped electrons. The main problem for electron tunneling is the positions of energy levels of electron trap and the excited state of luminescence center. It can be noted the  $Eu^{2+}$  excitation spectrum is a complex wide band covering range from 2.76 eV up to 4.96 eV (450 nm–250 nm) [1,6,13,19], the high frequency side of this band is due to charge transfer from oxygen to Eu, the low frequency side is determined by split 4f and 5d states of Eu, therefore, in accordance with *ab initio* calculations for two different cation sites [25, 26] there is a number of mutually close located energy levels within  $\sim 1$  eV interval. The study of  $Dy^{3+}$  doped YAG showed that there are 7 energy levels in the range 3.024–3.815 eV (with a difference of 0.79 eV) [16,21]. This suggests that the similar closely located Dy levels could be present in  $SrAl_2O_4$  as well. Therefore, if the energy of electron located at a trap is within the mentioned energy range of Eu and Dy ions energy levels, the tunneling probability is substantial.

The prior discussion leads to the conclusion that observed luminescence bands peaking at 457 nm, 526 nm and  $\sim 572$  nm in afterglow spectrum at 10 K arises from decay of excited  $Eu^{2+}$  and  $Dy^{3+}$  centers created via electron tunneling from host trap to  $Eu^{3+}$  and  $Dy^{4+}$  ions.

#### 4. Conclusions

The line groups visible under X-ray excitation in  $SrAl_2O_4:Eu$ , Dy material along with the typical  $Eu^{2+}$  broad emission band are attributed  $Dy^{3+}$  luminescence. Both Eu and Dy luminescence peaks are visible in the afterglow and TSL measurement. Based on TSL and time resolved spectral measurements we conclude, that under X-ray irradiation  $Eu^{2+}$  and  $Dy^{3+}$  serve as hole traps and the  $Eu^{3+}$  as well as  $Dy^{4+}$  are accumulated. Electron traps are located relative to  $Eu^{3+}$  and  $Dy^{4+}$  in such way, that electron tunneling probability is substantial. The afterglow in low temperatures, TSL measurements and the charging of luminescence intensity imply that electron tunneling is present in both  $SrAl_2O_4:Eu$ , Dy and  $SrAl_2O_4:Dy$ , and luminescence afterglow at 10 K arises from decay of excited  $Eu^{2+}$  and  $Dy^{3+}$  centers created via electron tunneling from host trap to  $Eu^{3+}$  and  $Dy^{4+}$  ions.

#### Acknowledgements

This research project was supported financially by ERDF Project No: Nr.1.1.1.1.16/A/182.

#### References

[1] K. Van den Eeckhout, P.F. Smet, D. Poelman, Persistent luminescence in  $Eu^{2+}$ -doped compounds: a review, *Materials* (Basel) 3 (4) (Apr. 2010) 2536–2566, <https://doi.org/10.3390/ma3042536>.

[2] D. Haranath, V. Shanker, H. Chander, P. Sharma, Tuning of emission colours in strontium aluminate long persisting phosphor, *J. Phys. D: Appl. Phys.* 36 (2003) 2244, <https://doi.org/10.1088/0022-3727/36/18/012>.

[3] C. Feldmann, T. Jüstel, C.R. Ronda, P.J. Schmidt, *Inorganic luminescent materials: 100 Years of research and application*, *Adv. Funct. Mater.* 13 (2003) 511–516, <https://doi.org/10.1002/adfm.200301005>.

[4] M. Sun, Z. Li, C. Liu, H. Fu, J. Shen, H. Zhang, Persistent luminescent nanoparticles for super-long time in vivo and in situ imaging with repeatable excitation, *J. Lumin.* 145 (2013) 838–842, <https://doi.org/10.1016/j.jlumin.2013.08.070>.

[5] E. Nakazawa, T. Mochida, Traps in  $SrAl_2O_4:Eu^{2+}$  phosphor with rare-earth ion doping, *J. Lumin.* 74 (1997) 236–237.

[6] J. Botterman, J.J. Joos, P.F. Smet, Trapping and detrapping in  $SrAl_2O_4:Eu,Dy$  persistent phosphors: influence of excitation wavelength and temperature, *Phys. Rev. B Condens. Matter* 90 (8) (2014) 1–15, <https://doi.org/10.1103/PhysRevB.90.085147>.

[7] W. Jia, H. Yuan, L. Lu, H. Liu, W.M. Yen, Phosphorescent dynamics in  $SrAl_2O_4:Eu^{2+}, Dy^{3+}$  single crystal fibers, *J. Lumin.* 3 (97) (1998) 0–4, [https://doi.org/10.1016/S0022-2313\(97\)00230-5](https://doi.org/10.1016/S0022-2313(97)00230-5).

[8] T. Aitasalo, J. Hölsä, H. Jungner, C.J. Krupa, M. Lastusaari, J. Legendziewicz, J. Niittykoski, Effect of temperature on the luminescence processes of  $SrAl_2O_4:Eu^{2+}$ , *Radiat. Meas.* 38 (4–6) (2004) 727–730, <https://doi.org/10.1016/j.radmeas.2004.01.031>.

[9] T. Aitasalo, J. Holsa, M. Lastusaari, J. Niittykoski, Mechanisms of persistent luminescence in  $Eu^{2+}, RE^{3+}$  doped alkaline earth aluminates, *J. Lumin.* 94–95 (2001) 59–63.

[10] P. Dorenbos, Mechanism of persistent luminescence in  $Eu^{2+}$  and  $Dy^{3+}$  codoped aluminate and silicate compounds, *J. Electrochem. Soc.* 152 (7) (2005) H107, <https://doi.org/10.1149/1.1926652>.

[11] K. Korthout, K. Van Den Eeckhout, J. Botterman, S. Nikitenko, D. Poelman, P.F. Smet, Luminescence and x-ray absorption measurements of persistent  $SrAl_2O_4:Eu, Dy$  powders: evidence for valence state changes, *Phys. Rev. B Condens. Matter* 85140 (2011) 1–7, <https://doi.org/10.1103/PhysRevB.84.085140>.

[12] F. Clabau, X. Rocquefelte, P. Denieard, S. Jobic, M. Whangbo, A. Garcia, T. Mercier, On the phosphorescence mechanism in  $SrAl_2O_4:Eu^{2+}$  and its codoped derivatives, *Solid State Sci.* 9 (2007) 608–612, <https://doi.org/10.1016/j.solidstatesciences.2007.03.020>.

[13] H. Hagemann, D. Lovy, S. Yoon, S. Pokrant, N. Gartmann, B. Walfort, J. Bierwagen, Wavelength dependent loading of traps in the persistent phosphor  $SrAl_2O_4:Eu^{2+}, Dy^{3+}$ , *J. Lumin.* 170 (2015) 299–304, <https://doi.org/10.1016/j.jlumin.2015.10.035>.

[14] V. Liepina, D. Millers, K. Smits, Tunneling luminescence in long lasting afterglow of  $SrAl_2O_4:Eu,Dy$ , *J. Lumin.* 185 (2017), <https://doi.org/10.1016/j.jlumin.2017.01.011>.

[15] A.N. Yerpude, S.J. Dhole, Optik Luminescence in trivalent rare earth activated  $Sr_4Al_2O_7$  phosphor, *Opt. - Int. J. Light Electron Opt.* 124 (18) (2012) 3567–3570, <https://doi.org/10.1016/j.ijleo.2012.11.064>.

[16] M. Ayvaci, A. Ege, N. Can, Radioluminescence of  $SrAl_2O_4:Ln^{3+}$  ( $Ln = Eu, Sm, Dy$ ) phosphor ceramic, *Opt. Mater.* 34 (2011) 138–142, <https://doi.org/10.1016/j.optmat.2011.07.023>.

[17] D. Nakachi, G. Okada, M. Koshimizu, T. Yanagida, Storage luminescence and scintillation properties of Eu-doped  $SrAl_2O_4$  crystals, *J. Lumin.* 176 (2016) 342–346, <https://doi.org/10.1016/j.jlumin.2016.04.008>.

[18] F. Clabau, et al., Mechanism of phosphorescence appropriate for the long-lasting phosphors  $Eu^{2+}$ -doped  $SrAl_2O_4$  with codopants  $Dy^{3+}$  and  $B^{3+}$ , *Chem. Mater.* 17 (2005) 3904–3912, <https://doi.org/10.1021/cm050763r>.

[19] H.M. Poort, W.P. Blokpoel, G. Blasse, Luminescence of  $Eu^{2+}$  in barium and strontium aluminate and gallate, *Chem. Mater.* (15) (1995) 1547–1551, <https://doi.org/10.1021/cm00056a022>.

[20] P.J.R. Montes, M.E.G. Valerio, Radioluminescence properties of rare earths doped  $SrAl_2O_4$  nanopowders, *J. Lumin.* 130 (2010) 1525–1530, <https://doi.org/10.1016/j.jlumin.2010.03.024Get>.

[21] P.J.R. Montes, M.E.G. Valerio, M.V.S. Rezende, Mechanisms of radioluminescence of rare earths doped  $SrAl_2O_4$  and  $Ca_{12}Al_4O_{33}$  excited by X-ray, *J. Electron. Spectrosc. Relat. Phenom.* (189) (2013) 39–44, <https://doi.org/10.1016/j.jelspec.2013.06.011>.

[22] G. Raju, H. Jung, J. Park, J. Chung, B. Moon, J. Jeong, S. Son, J. Kim, Sintering temperature effect and luminescent properties of  $Dy^{3+}$ : YAG nanophosphor, *J. Optoelectron. Adv. Mater.* 12 (6) (2010) 1273–1278.

[23] G.S. Raju, J. Park, H. Jung, B. Moon, J. Jeong, J. Kim, Luminescence properties of  $Dy^{3+}$ :  $GdAlO_3$  nanopowder phosphors, *Curr. Appl. Phys.* 9 (2009) 92–95.

[24] T. Takeyama, T. Nakamura, N. Takahashi, M. Ohta, Electron paramagnetic resonance studies on the defects formed in the  $Dy(III)$ -doped  $SrAl_2O_4$ , *Solid State Sci.* 6 (2004) 345–348, <https://doi.org/10.1016/j.solidstatesciences.2004.02.001>.

[25] M. Nazarov, M.G. Brik, D. Spassky, B. Tsukerblat, A. Nor Nazida, M.N. Ahmad-Fauzi, Structural and electronic properties of  $SrAl_2O_4:Eu^{2+}$  from density and functional theory calculations, *J. Alloys Compd.* 573 (2013) 6–10, <https://doi.org/10.1016/j.jallcom.2013.04.004>.

[26] M. Nazarov, M.G. Brik, D. Spassky, B. Tsukerblat, Crystal field splitting of 5d states and luminescence mechanism in  $SrAl_2O_4:Eu^{2+}$  phosphor, *J. Lumin.* 182 (2017) 79–86, <https://doi.org/10.1016/j.jlumin.2016.10.015>.